The Crucial Role of Water on the Stability and Electrocatalytic Activity of Pt Electrodes

Johanna Ranninger[a,b,*], Karl J.J. Mayrhofer[a,b], Balázs B. Berkes,[a,*]

[a] Helmholtz Institute Erlangen-Nürnberg for Renewable Energy (IEK-11), Forschungszentrum Jülich GmbH, 91058 Erlangen, Germany

[b] Department of Chemical and Biological Engineering, Friedrich-Alexander-Universität Erlangen-Nürnberg, 91058 Erlangen, Germany

ABSTRACT: Understanding the role of water on the activity and stability of electrocatalysts is of great interest for different fundamental reactions. Investigations aiming to expand understanding of this are very challenging in aqueous electrolytes. By contrast, nonaqueous electrolytes with very well defined water content can provide ideal conditions to better clarify the role of water in electrochemical reactions. In this paper, the dissolution and electrochemical behavior of Pt during potentiodynamic and potentiostatic measurements in methanol-based and acetonitrile-based electrolytes with accurately controlled water content of <1 ppm, 100 ppm, 1000 ppm, 1 %, and 10 % are studied. In methanol-based electrolytes, we demonstrate the promoting effect of small amounts of water on the methanol oxidation reaction. We show the formation of surface oxide species with increasing water content in the Pt dissolution profile, which develops from a purely anodic to a predominantly cathodic dissolution, a known characteristic of aqueous electrolytes. The effect of water on the electrode stability is fundamentally different in acetonitrile-based systems: presumably, the strong adsorption of solvent molecules competes with the adsorption of water and thus inhibits the formation of an oxide layer at the surface even up to a water concentration of 1 % as revealed by potentiodynamic measurements.

1. INTRODUCTION

The use of nonaqueous electrolytes bears many advantages over classical water-based electrochemistry, like wider electrochemical stability windows of solvents, increased chemical stability of alkali metals, greater solubility of certain chemical compounds, and huge variability of the physico-chemical properties of varying solvents. The development of new battery systems[1] and a renaissance of organic electrosynthesis[2, 3] in recent decades has provoked renewed interest in understanding processes at the electrode interface in nonaqueous electrolytes and the effect of the presence of trace amounts of water. Compared to studies of aqueous electrocatalysis, studies in nonaqueous media that focus on activity-promoting effects and electrode stability are scarce but no less important.

Few mechanistic studies of oxygen and hydrogen conversion reactions have been performed in nonaqueous electrolytes. For example, the oxygen reduction reaction (ORR) has been studied in different organic electrolytes to identify appropriately active electrode materials and electrolyte composition for metal-air batteries.[4-8] Other studies investigated hydrogen oxidation/evolution to elucidate general reaction mechanisms.[9-12] One key question in those studies is the role of water at the electrode material—electrolyte interface as a reactant, decoupled from its function as a solvent in aqueous media.[4, 9-13] The concept of controlled addition of water to nonaqueous electrolytes can provide essential insights into mechanistic concepts. Pemberton et al. proposed almost 30 years ago that water molecules cluster around supporting electrolyte ions and can be transported dependent on the potential to the electrode interface in butanol-based electrolytes. This propensity leads to the conclusion that water is not homogeneously distributed in the system but can be present in higher concentrations at the interface compared to the bulk electrolyte.[14] This observation shows the difficulties and challenges in mapping the electrochemical characteristics of truly nonaqueous systems not skewed by water. Recently, Dubouis et al. explained that coordinated water is more easily reduced compared to free water. They demonstrated this by measuring hydrogen reduction on a Pt electrode in acetonitrile—water mixtures with $LiClO_4$, $NaClO_4$ and $TBAClO_4$ (TBA: tetrabutylammonium) as supporting electrolytes. $LiClO_4$ and $NaClO_4$ improved the HER by facilitating the transport of water to the electrode surface because of the high hydrophilicity of the Li^+ and Na^+ ions, forming a large hydration shell around the ions (resulting from their large ionic potentials). By contrast, the bulky, hydrophobic TBA^+ cation suppressed HER.[11, 12] In other

situations, there may be no water present at the interface at certain potentials, in which case the interface is dominated by the presence of hydrophobic ions. Feng et al. have demonstrated this kind of interface tuning for room temperature ionic liquids by applying molecular dynamic simulations.[15]

Ions in the form of supporting electrolytes or impurities are not the only factor affecting the transport of water molecules to the surface and influencing their reactivity. Different solvent molecules also interact differently with the electrode surface and affect water adsorption. Więckowski classified the solvent adsorption onto a Pt electrode into three classes: (i) a surface—solvent complex bond resulting from the solvent π orbitals overlapping with d-orbitals of the metal (ii) adsorption of solvent molecules into the second ad-layer (iii) adsorption of solvent molecules also into the second ad-layer reacting with chemisorbed water.[16]

Acetonitrile, found in the first group[16], is often used as a solvent for fundamental reactivity studies due to its simple chemical structure, wide electrochemical stability window, good miscibility with water, relatively good conductivity, and capability to solvate ions (εr = 37.5).[10, 13, 17-20] Different analysis tools like *in situ* infrared spectroscopy[19, 21, 22], surface-enhanced Raman spectroscopy[23, 24], and surface X-ray diffraction[20] were used to investigate the adsorption behavior, decomposition, and influence of water on the acetonitrile—Pt interaction. It has been shown that acetonitrile chemisorbs at the Pt surface, being able to displace water and undergo oxidation and reduction without being desorbed from the surface within a wide potential range.[17, 21] Baldelli et al. showed using sum-frequency generation that acetonitrile undergoes a reorientation on Pt at the potential of zero charge (pzc). Positive of pzc the nitrile (CN) group faces the Pt surface, and negative of pzc the methyl (CH_3) group faces the Pt surface. This reorientation is enhanced with small amounts of water but disrupted above around 5 mol% of water.[25] Furthermore, Harlow et al. showed that an increasing concentration of acetonitrile in an aqueous electrolyte leads to a more compact double layer structure and increasing Pt surface expansion.[20] It is well known from literature that the addition of water decreases the electrochemical stability window, although the reductive decomposition was investigated in more detail compared to oxidative decomposition. The reductive decomposition of acetonitrile on roughened Pt was reported to result in adsorbed CN and CH_3 groups.[23, 24] It was also found that acetonitrile can undergo a reductive dimerization- and trimerization reaction, leading to cyclic products like 4-amino-2,6-dimethylpyrimidine or 2,4,6-trimethyl-1,3,5-triazine, but methane was also described as reduction product.[26, 27] For anodic degradation, it was found that upon the addition of water the potential window is decreased and anodic acetonitrile decomposition is induced by water oxidation forming $H_2O^{+\cdot}$. $H_2O^{+\cdot}$ can react with acetonitrile to form acetamide, which can further decompose to CO, CO_2, methanol, methane, acetic acid and formic acid. Depending on the nature of the supporting electrolyte and water content, the formation of an acetonitrile dimer or polyacetonitrile is also possible.[22, 28]

Methanol is classified in group (iii) regarding solvent—Pt interaction according to Więckowski[16], as it is not able to displace instead reacts with chemisorbed water at the electrode surface to form a strong ad-layer. Methanol adsorption has also been of interest for a long time with the goal of understanding methanol oxidation reaction (MOR) mechanisms. Different routes leading to oxidation products like CO_2, formaldehyde, and formic acid were outlined, and OH_{ad} species were identified as playing a crucial role in the oxidative decomposition of methanol.[29-31] A recent study showed that an increased water concentration in methanol shifts the onset potential for methanol oxidation reaction to more negative potentials because of the higher concentration of OH_{ad} species and free Pt sites.[32]

In our previous works, we have presented a method, for on-line investigation of noble metal electrode dissolution during electrochemical measurements by coupling an electroanalytical flow cell (EFC) with an inductively coupled plasma mass spectrometer (ICP-MS). The very high sensitivity and potential resolution of the method (quantification limit: dissolution of 0.13 monolayers of Pt within one hour) indirectly give information about ongoing surface processes, like oxide formation or any blocking effect of adsorbed species by detecting dissolved Pt.

Pt dissolution was compared in aqueous and methanol-based media, whereby it was shown that Pt dissolution in methanol-based media is governed by anodic dissolution.[33] In aqueous electrolytes, on the contrary, Pt only slightly dissolves directly during the anodic going scan, owing to the forming protective Pt oxide layer, which is dissolved in the cathodic scan representing the main dissolution pathway in aqueous electrolytes.[34-36] Furthermore, we have shown that Pt dissolution exhibits striking differences in anhydrous methanol-based and acetonitrile-based electrolytes at elevated temperatures due to oxidation intermediates and products formed from methanol and the complexing behavior of acetonitrile, while still only exhibiting anodic dissolution.[37]

In this paper, we show new aspects of the electrochemical and dissolution behavior of Pt in methanol-based and acetonitrile-based electrolytes, while precisely controlling their water content through on-line monitoring of Pt dissolution in cyclic voltammetric and chronoamperometric measurements. The expected shift from a purely anodic dissolution, typical for water-free electrolytes, to a predominantly cathodic one, characteristic for aqueous electrolytes, is only observed in methanol-based electrolytes. In acetonitrile, higher water concentration is required to suppress anodic dissolution and provoke cathodic dissolution. This behavior is in agreement with the above-described surface adsorption processes. In this study, we only use $LiClO_4$ as supporting electrolyte, noting that other supporting electrolytes, as discussed above, might drastically influence the adsorption of water and solvent molecules and, hence, the electrochemistry of Pt.

2. EXPERIMENTAL METHODS

The Pt dissolution profiles and the corresponding cyclic voltammetry and chronoamperometry measurements presented herein were obtained using an electroanalytical flow cell (EFC)

coupled to an ICP-MS, which was previously described.[33] All sample preparation procedures, water content determination, and electrochemical measurements were carried out in an argon-filled glovebox (MBRAUN) where H_2O and O_2 levels were kept < 0.1 ppm.

Anhydrous methanol-based and acetonitrile-based electrolytes were prepared after careful solvent purification[37], starting with dry methanol (max. water content 0.003 %, SeccoSolv, Merck) and acetonitrile (water content max. 0.001 %, VWR Chemicals). The purified solvents were mixed with $LiClO_4$ (battery grade, dry, 99.99 % trace metals basis, Sigma Aldrich) dried under vacuum at 60 °C for at least three days. Electrolytes with a water content of 100 ppm, 1000 ppm, 1 % and 10 % by weight were prepared by either adding water directly to the electrolyte or adding a stock solution containing a well-defined amount of water (1:10). The water concentration of electrolyte solutions (the solvent together with the conducting salt) with different water contents was determined using Karl Fischer titration (917 Coulometer, Metrohm). The accuracy of water contents stated in this article is ± 5 %.

All electrochemical measurements were conducted using a VSP 300 potentiostat (Biologic). A 25 µm-thick Pt foil (polycrystalline Pt 99.99 %, MaTecK), and a glassy carbon rod (HTW Hochtemperatur-Werkstoffe GmbH) were used as working electrode (WE) and counter electrode (CE), respectively. The Pt foil was polished with 0.3 µm Al_2O_3 paste on polishing cloth MD-Mol (Struers) before each use. The CE, EFC, fittings, and tubing were cleaned in ethanol, isopropyl alcohol, and acetone in an ultrasonic bath and dried overnight at 60 °C in a VO400 vacuum oven (Memmert GmbH & Co. KG). As the reference electrode, a homemade nonaqueous reference electrode was prepared. For that purpose, a silver wire was immersed in an electrode body with leakage-free frit (purchased from Innovative Instruments Inc.) filled with MeOH or MeCN containing 0.1 mol L^{-1} tetrabutylammonium perchlorate and 0.01 mol L^{-1} $AgNO_3$. The RE potential was calibrated before measurements in an electrolyte solution containing ferrocene and all potentials are referenced against the ferrocene/ferrocenium (Fc/Fc^+) couple (Fc/Fc^+ to SHE: +0.624[38]). With each new water content, electrochemical impedance was measured to estimate the solution resistance, R_u. The R_u was determined to be around 200 Ω for MeCN-based electrolytes and 550 Ω for MeOH-based electrolytes. The electrochemical measurements were manually compensated with 85 % of the determined resistance in case of MeOH-based electrolytes. The very low current values measured in MeCN-based electrolytes do not justify the need for IR compensation. During the measurements the temperature of the working electrode was kept at 25 °C and the electrolyte was pumped through the EFC with a flow rate of 150 µL min^{-1} using a Legato® 100 syringe pump. The EFC outlet was directly connected to the ICP-MS (NexION 2000, PerkinElmer) located outside of the glovebox. An internal standard consisting of 10 µg L^{-1} Re (from $(NH_4)ReO_4$ in water (Certipur®, Merck)), 1 v/v% HNO3 in ethanol for the MeOH-based electrolyte and in water for the MeCN-based electrolyte was added with approximately 150 µL min^{-1} using the built-in MP2 peristaltic pump.

Analyzing organic samples in an ICP-MS requires the sample uptake rate into the plasma to be lowered due to the high vapor pressure of organic solvents compared to aqueous-based electrolytes. This is achieved by reducing the inner diameters for the tubing and injector, as well as cooling the spray chamber. Furthermore, O_2 needs to be added to oxidize organic matrices to CO_2 and prevent soot formation on the orifices of the cones, which leads to cone blockage, in turn resulting in unstable measurements or measurement interruption.[18, 39, 40] The optimal parameters have to be individually identified for each electrolyte system. The ICP-MS parameters used were a spray chamber temperature of 2 °C, a radio frequency power of 1600 W, an injector diameter of 1.5 mm, a nebulizer gas flow of 0.88 L min^{-1} and an O_2 gas flow of 0.07 L min^{-1} for MeCN-based and nebulizer gas flow of 0.98 L min^{-1} and O_2 gas flow of 0.08 L min^{-1} for MeOH-based electrolytes. The instrument was calibrated before measurements with an aqueous Pt standard (H_2PtCl_6 in HCl 7% 1000 mg/l Pt Certipur®, Merck) with concentrations of 0.5 µg L^{-1}, 1 µg L^{-1} and 5 µg L^{-1} dissolved in the respective electrolyte matrix.

3. RESULTS AND DISCUSSION

3.1. The effect of water on the potentiodynamic dissolution of Pt

Cyclic voltammograms (CVs) of Pt with different water contents were measured with 5 mV s^{-1} between –0.5 V and 0.9 V after performing 50 cleaning cycles with 200 mV s^{-1}. In the selected potential range, methanol oxidation takes place but 0.9 V vs. Fc/Fc^+ is well below the potential at which oxidative acetonitrile decomposition occurs. In order to calculate current densities, the geometric surface area (4.33 mm^2) was used, which represents the contact area of the EFC with Pt. CVs of Pt and corresponding dissolution profiles in MeOH-based and MeCN-based electrolytes (MeOH and MeCN containing 0.05 mol L^{-1} $LiClO_4$) are shown in Fig. 1.

Even though purification of solvents was carried out under inert conditions with great care and the measured water content was below the detection limit of 1 ppm using highly sensitive coulometric Karl Fischer titration, up to 6.7×10^{13} water molecules (4.4×10^{-8} mol mL^{-1}) enter the flow channel during one second in our system, considering the flow rate of 150 µL min^{-1} and 1 ppm as the limit of detection for the Karl Fischer titration. Only a small portion of these molecules is capable of reacting, i.e. those within the diffusion layer at the electrode. Meanwhile, 1.9×10^9 Pt atoms per second need to reach the ICP-MS to be quantified (flow rate: 150 µL min^{-1}, limit of quantification: 0.25 ppb), meaning that even if a minimal fraction of residual water reacts at the surface, the analytical method is sensitive enough to detect subtle differences in Pt dissolution behavior.

In the dissolution profile of Pt in the anhydrous MeOH-based electrolyte (Fig. 1a), only anodic dissolution is observed, which occurs during the forward scan and has been described in our previous works.[33, 37] At only 100 ppm of water, a shoulder appears in the dissolution profile, which becomes more pronounced at 1000 ppm and exceeds anodic dissolution at a water content of 1 %. At 10 % water concentration, the characteristic Pt dissolution in

aqueous electrolytes emerges, where the anodic dissolution is hindered (see also Fig. 4), while protective Pt-oxide species are formed at the surface and the main dissolution pathway, associated with the reduction of the oxidized Pt surface, cathodic dissolution, is observed in the reverse scan.[36] The stability behavior of Pt in PtRu electrocatalysts was investigated in acidic and alkaline electrolytes in the presence of methanol due to its optimized activity for MOR and the applicability of this bifunctional catalyst for direct methanol fuel cells. Ru increases the availability of oxygenated species at the surface and facilitates the early onset of MOR and the oxidative removal of poisonous species from the catalyst surface. It was found that Pt dissolution behavior is similar in Pt/C and PtRu/C and that the presence of methanol in aqueous electrolytes affects the dissolution of Pt from the bifunctional PtRu catalysts only slightly.[41, 42] The marginally enhanced dissolution found by Jovanovič et al. is explained by the formation of CO intermediates[41] and the slightly decreased dissolution is explained by the stabilizing effects of reaction intermediates found by Kormányos et al.[42]. Despite contradicting observations regarding the exact influence of reaction intermediates, the shape of the Pt dissolution curve and the dissolved amount in a MeOH-based electrolyte containing 10 % water in our study are comparable with that observed for Pt in acidic media with and without methanol present. Increasing the water content significantly changes the shape of the CVs, as well. Firstly, MeOH oxidation onset potentials shift to more negative values, as has been described previously. This phenomenon is explained by the promoting effect of water on MOR.[32] In aqueous electrolytes, the rate-determining step at lower potentials between 0.5 V and 0.7 V vs. RHE is the oxidative removal of oxidized reaction intermediates at the surface.[43] In this potential region, oxygenated species at the electrode surface are essential for the MOR and are mainly formed by water reacting with the surface.[44, 45] At higher potentials, the reaction of water at the electrode surface and formation of Pt-O species becomes more favorable and adsorption of MeOH becomes rate-determining[46], which leads to the declining current between 0.4 and 0.5 V vs. Fc/Fc^+ at 10 % water concentration. The shift in the onset potential is most significant from 1 % to 10 % water content, probably because the concentration of oxygenated species at the electrode surface at low potentials is not high enough to significantly enhance the rate of MOR at lower water concentrations. Sufficient coverage of the surface with oxygenated species in order to shift the onset potentials to more negative values is only reached if the water content is higher than 1 %.

The effect of water concentration, even at lower water contents, on the peak potential of the peak in the reverse scan is much more pronounced and also shifts to more negative potentials with increasing water concentration. This peak is associated with MeOH oxidation on the freshly reduced Pt surface.[47] This shift is an expected observation, since the overpotential for the reduction of Pt oxide species increases as a more stable Pt oxide layer forms during the anodic scan, which is the case for higher water contents. It is also noticeable that for water concentrations <1 ppm, 100 ppm, or 1000 ppm, the current density in the reverse scan is higher than in the forward scan, which indicates a promoting effect of reaction intermediate adsorption on MOR, whereby the absolute measured charge is highest with a water concentration of 100 ppm. At 100 ppm, oxygenated species are already present at the surface in small concentrations to facilitate MOR but not enough to form a stable Pt oxide layer, which could passivate the surface, providing seemingly ideal conditions for MOR within the studied potential range. We can conclude in the case of MeOH-based electrolyte that the addition of water leads to the gradual adsorption of oxygenated species on the Pt surface and the formation of a Pt oxide layer, which is reduced at lower potentials in the reverse scan of the CV and observed in the dissolution profile as cathodic dissolution. Even low water content seems to have a promoting effect on MOR but not enough to drastically shift onset potentials to more negative values, as this is observed only for a water content of 10 %.

We can make a completely different observation when performing the same experiments in acetonitrile-based electrolytes. An increasing water content shows no significant influence on the Pt dissolution in CVs up to 1000 ppm water (see Fig. 1c and 1d). For water content of <1 ppm, 100 ppm, and 1000 ppm, only anodic dissolution is observed with similar amounts of dissolved Pt (see Fig. 1c). The corresponding CVs are featureless, showing mainly non-faradaic processes in the applied potential range (see Fig. 1d). At 1 % water content, a shoulder develops in the Pt dissolution profile during the reverse scan, indicating the start of cathodic dissolution, which also means that some Pt oxide species are formed in the anodic scan. This finding is in accordance with the increasing observable current densities measured in the CVs. The Pt oxide formation becomes more pronounced at 10 % water content, where two similarly shaped peaks are observed in the dissolution profile along with further increasing current densities. The CV starts to resemble a CV in aqueous electrolytes, even though the characteristics are not yet clearly pronounced. On the CV curve, measured in acetonitrile containing 10 % water, the increase in anodic current starts at 0.35 V, which corresponds to the oxidation of the Pt surface, and an increasing cathodic current at 0.25 V in the reverse scan, indicates the reduction of Pt oxide.

The striking differences in the water-dependent Pt dissolution behavior lead us to conclude that passivation of Pt in the form of Pt oxide species occurs differently in methanol and acetonitrile. One explanation supported by previous findings might be the strong adsorption of acetonitrile molecules on the Pt electrode surface. Shayehi et al. found based on single crystal adsorption calorimetry (SCAC) measurements that the heat of adsorption at zero-coverage limit for acetonitrile is –103 kJ mol^{-1} on Pt (111) at 300 K.[48] Karp et al. determined a value of –60.5 kJ mol^{-1} for the heat of adsorption for methanol on Pt (111) at zero-coverage limit at 100 K and 150 K in SCAC studies.[49] The stronger binding energy between solvent molecules in MeCN-based compared to MeOH-based electrolyte prevents water molecules from reaching the surface at low water concentrations (100 ppm, 1000 ppm) and also explains how the difficulty in displacing acetonitrile from the Pt surface cause cathodic dissolution to develop very slowly at higher water contents (1 %, 10 %). The adsorption of methanol on Pt, on the other hand, is not strong enough to hinder water adsorption even with small amounts, which is supported by the fast development of cathodic

dissolution and the shift of peak potentials in the forward and reverse scans.

Due to the strong adsorption of acetonitrile on the Pt electrode and its effect on the competitive adsorption of oxygenated species observed during these measurements, it is questionable if electrolyte systems based on acetonitrile are suitable for fundamental mechanistic studies of e.g. hydrogen or oxygen conversion reactions. The strong adsorption of the solvent molecules themselves might interfere with the adsorption of reactive species and the usefulness of conclusions drawn from those studies related to aqueous electrolytes systems might be limited.

The potential limits for the measurements shown in Fig. 1 were chosen because of severe gas evolution (H_2 at the CE and CO or CO_2 on the WE depending on the water content) due to methanol decomposition at higher potentials, interrupting the contact of the electrodes during the measurement. For the sake of comparability, we chose the same potential limits for the MeCN-based electrolyte, although the potential window could be extended in this case due to the excellent electrochemical stability of acetonitrile. When performing experiments in an extended potential range, i.e. between –0.5 V and 1.3 V vs. Fc/Fc^+, a very similar picture emerges (see Fig. 2). Even though a higher Pt dissolution is measured in total, the shape of the dissolution curves, as well as CVs, fundamentally remain the same, indicating that adsorption of MeCN still prevails with increasing potential. The dissolution is only slightly enhanced at low water contents (100, 1000 ppm), and only anodic dissolution is observable. However, very low current densities are still obtained from the Pt CVs. At 1 % water content, a shoulder representing cathodic dissolution appears on the dissolution profile and at 10 %, two similarly shaped peaks can be observed. Along with these changes at higher water contents (1 %, 10 %), the measured current densities significantly increase.

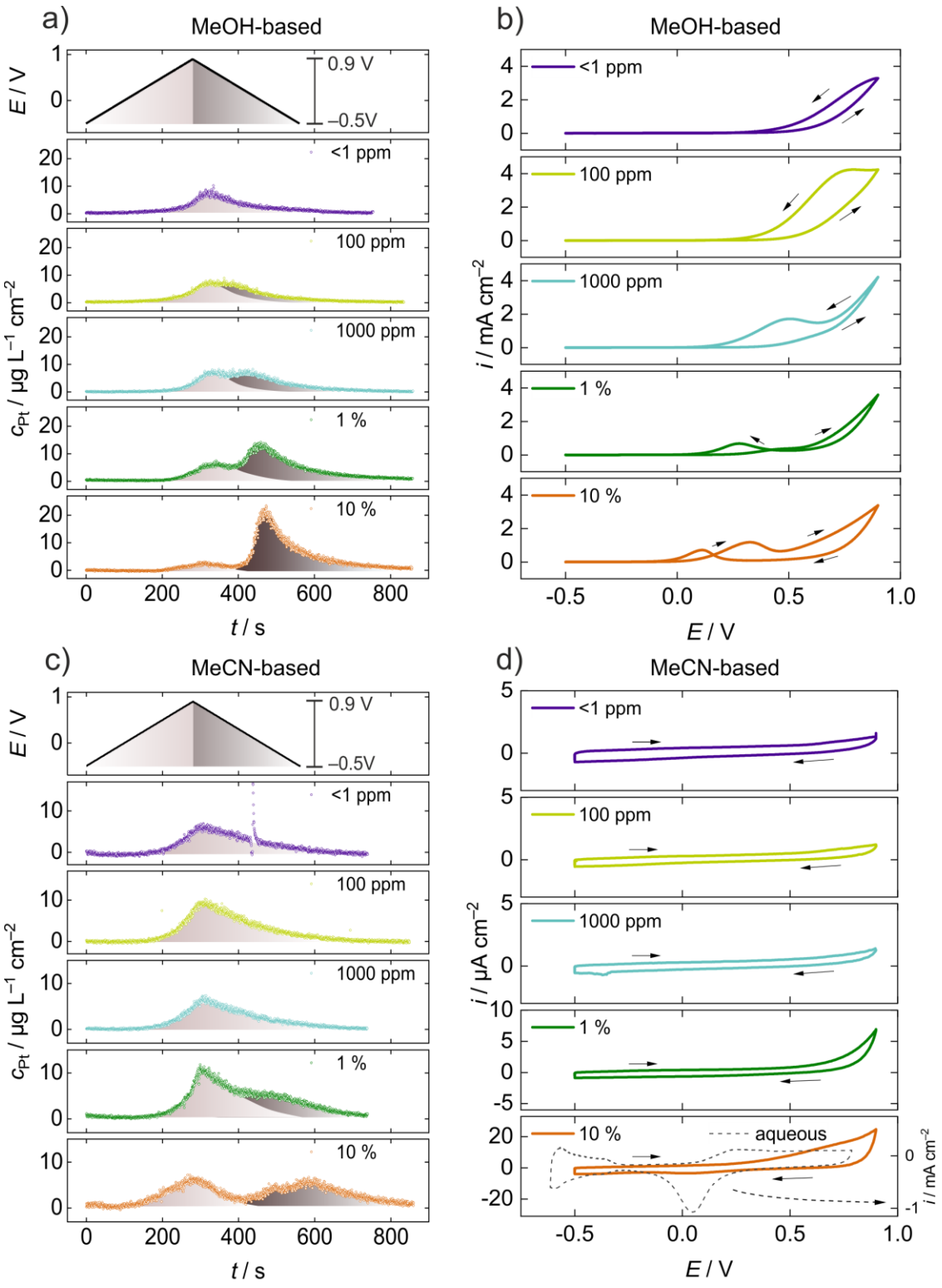

Fig. 1: Pt dissolution vs. time with different water contents (<1 ppm, 100 ppm, 1000 ppm, 1 %, 10 %) in a) 0.05 mol L^{-1} $LiClO_4$ containing MeOH and c) 0.05 mol L^{-1} $LiClO_4$ containing MeCN electrolytes and current density vs. potential in b) 0.05 mol L^{-1} $LiClO_4$ containing MeOH and d) 0.05 mol L^{-1} $LiClO_4$ containing MeCN obtained during cyclic voltammetry between –0.5 V vs. Fc/Fc^+ and 0.9 V vs. Fc/Fc^+ with 5 mV s^{-1}. The dashed line in Fig. 1d on the 10 % water content curve represents a CV in aqueous $HClO_4$ (note the different current scales). In Fig. 1c the spike in the ICP-MS signal at a water concentration of <1 ppm around 430 s is caused by a small bubble in the system (artefact).

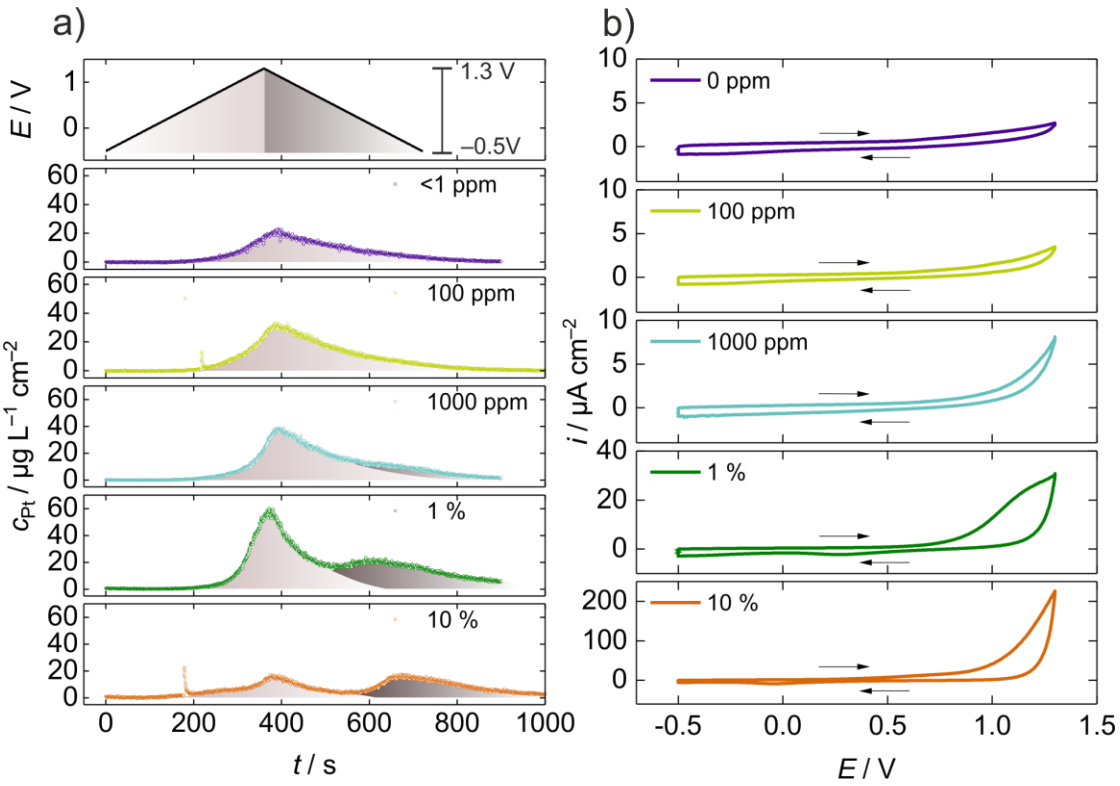

Fig. 2: a) Pt dissolution vs. time and current density vs. potential obtained in 0.05 mol L^{-1} $LiClO_4$ containing MeCN with different water contents (<1 ppm, 100 ppm, 1000 ppm, 1 %, 10 %) during cyclic voltammetry between –0.5 V vs. Fc/Fc^+ and 1.3 V vs. Fc/Fc^+ with 5 mV s^{-1}. In Fig. 2a the spikes in the ICP-MS signal at water concentrations of 100 ppm and 1 % are caused by small bubbles in the system (artefacts).

The obtained Pt dissolution curves were integrated and the total dissolved amounts (TDA) of Pt calculated for the studied electrolyte systems in the applied potential limits (see Fig. 3). The TDAs were calculated from at least three measurements and the standard deviations are indicated as error bars in Fig. 3a. Similar trends are observed for MeOH-based and MeCN-based electrolytes (–0.5 V – 1.3 V), namely the increase in TDA from <1 ppm to 1 % water content followed by a decrease in TDA for 10 % water content (see Fig. 3a). For methanol (grey bares in Fig. 3), this observation can be explained by the increasing cathodic dissolution starting from 100 ppm water content, while anodic dissolution remains at a high rate. The oxide layer formed at the Pt surface only partly suppresses anodic dissolution even at water contents as high as 10 % when cathodic dissolution becomes the predominant dissolution mechanism. In the case of MeCN-based electrolyte during CVs with an upper potential limit of 1.3 V (green bars in Fig. 3), the anodic Pt dissolution increases with increasing water content up to 1 %, where cathodic dissolution starts to appear. The reasons for increased anodic dissolution with increasing water content might be the destabilization of adsorbed acetonitrile and the top Pt layer at the electrode due to changes in the double layer structure. The observed difference in Pt TDA calculated from CVs between –0.5 and 0.9 V with varied water contents in MeCN-based electrolytes is much less pronounced. For low water contents (<1 ppm, 100 ppm, 1000 ppm), the dissolved amounts are very similar and only increase with high water contents (1 %, 10 %) when cathodic dissolution is observable. The measured anodic dissolution is generally very small for the MeCN-based electrolyte within this potential window. Slight variations in TDA cannot be clearly distinguished and changes are not significant.

Furthermore, the ratios of dissolution charge to total charge were calculated (see Fig. 3b). The dissolution charges were obtained from the TDAs, using Faraday's law under the assumption that Pt dissolution only occurs in a two-electron pathway. For the calculation of the total charge, the current vs. time curves were used. For the MeOH-based system the dissolution charge ratio (grey bars in Fig. 3b) follows the same trend as its corresponding calculated TDA. The reason for this is that increasing water content leads to a shift of the onset potential of the MOR to more negative values; however, the formation of oxide species on the surface inhibits the MOR at higher potentials, leveling the total charge to similar values for varying water contents. In acetonitrile-based electrolytes (blue and green bars in Fig. 3b), the Pt dissolution charge ratio is in the range of 0.2 % to 2.5 % because the measured currents are much lower than in methanol. Here, the addition of water in the concentration of 1 % and 10 % leads to a significant increase in current density. In the electrolyte containing 10 % water a 10-fold

and a 100-fold increase in the total charge is observed for CVs between –0.5 and 0.9 or 1.3 V, respectively, which results in a decreasing charge ratio for water concentrations of 1 % and 10 % water concentration. This means that the increased current is mostly related to other processes than Pt dissolution.

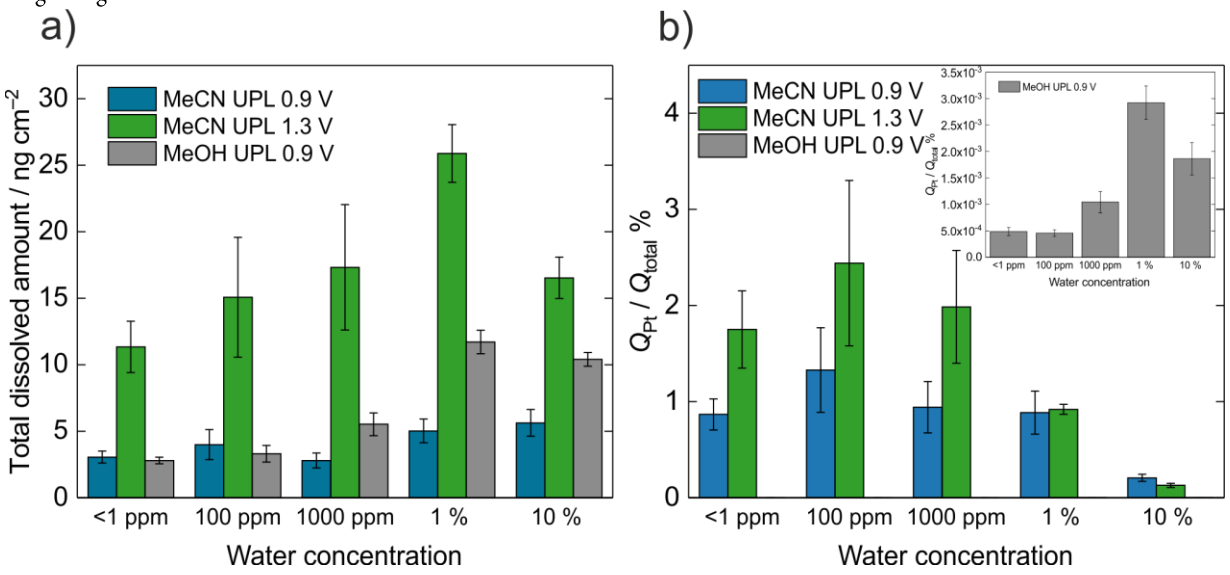

Fig. 3 Water-dependent total dissolved amounts and charge required for Pt dissolution related to total measured charge calculated from Pt dissolution and CV curves recorded between –0.5 V vs. Fc/Fc$^+$ and 0.9 V vs. Fc/Fc$^+$/1.3 V vs. Fc/Fc+ with 5 mV s^{-1} in 0.05 mol L^{-1} $LiClO_4$ containing MeOH and 0.05 mol L^{-1} $LiClO_4$ containing MeCN shown in Fig. 1 and 2.

3.2 The effect of water on the potentiostatic dissolution of Pt

Pt dissolution was also measured during chronoamperometry (CA) for the same MeOH-based and MeCN-based electrolytes. A potential of –0.5 V was applied for 30 s, followed by 7 min at 0.9 V and 2 min at–0.5 V again. Fig. 4a) and c) show Pt dissolution at the applied potentials in methanol and acetonitrile, respectively. In Fig. 4b) and d), current vs. time during the 0.9 V step is displayed. The current density values in Fig. 4b) and d) indicate the current density at the end of the potential step at 0.9 V. Qualitative assessment of anodic and cathodic dissolution in both electrolyte systems shows great similarities with Pt dissolution during potentiodynamic measurements. Cathodic dissolution in MeOH-based electrolyte develops steadily with increasing water content and for water contents of 1000 ppm and higher, the anodic dissolution is greatly hindered, presumably by the formation of a passivating layer of oxides, reflected in a decrease in the concentration vs. time curves. In the CA curves, the current density value at the end of 7 min at oxidative potentials decreases with increasing water content. In the curve at <1 ppm water concentration, the current density increases with time, supporting the theory of reaction intermediates having a promoting effect on the MOR. This initial current density increase can also be observed for 1000 ppm and 100 ppm, where the MOR rate is highest among all water contents after 180 s, followed by a decreasing current density due to passivation of the Pt surface resulting in a decreased rate of MOR on Pt oxide. For MeCN-based electrolytes, a decrease in anodic current and a peak for cathodic dissolution is only observable at a high water content of 1 % or 10 %. The significant increase in anodic dissolution for 1 % water concentration at the beginning of the potential step is of particular interest. One possible explanation might be the reorientation of the MeCN molecule around the potential of zero charge, which is disrupted at water concentrations of approximately 2 wt%.[25] Around 1 % water concentration might be enough to weaken the acetonitrile Pt adsorption strength and allow Pt dissolution, but not high enough to instantly form a Pt oxide layer, protecting the surface from anodic dissolution. Small peaks in the Pt dissolution profile also occur for low water concentrations (<1 ppm, 100 ppm, 1000 ppm) upon switching from oxidizing potentials to reducing potentials. This is associated with the dissolution of single Pt atoms at surface imperfections. All CA curves (Fig. 4d) exhibit a constantly decreasing current density with time, whereby the current densities are generally higher at higher water contents, similarly to the observations during CV measurements.

The most significant contrast in dissolution behavior appears at 10 % water content. When calculating the TDA for MeOH-based and MeCN-based electrolytes, the values are comparable with 6.2 ng cm^{-2} and 6.9 ng cm^{-2}, respectively. However, when assessing the anodic and cathodic dissolution individually, the ratio is roughly 1:4 for the MeOH-based and 1:1 for the MeCN-based system, illustrating the different preferences for forming Pt—O and dissolution mechanisms.

Another very striking difference arises when comparing the shape of the anodic dissolution profiles in the anhydrous (water content <1 ppm) electrolytes. Pt dissolution increases almost linearly when applying 0.9 V in the MeOH-based electrolyte, reaching a steady-

state value of around 20 $\mu g \cdot L^{-1} \cdot cm^{-2}$. We can speculate that this is caused by the formation of various oxidation products and the increasing availability of oxygenated species forming at the surface during electrolysis. As was described before, diverse MOR mechanisms lead to intermediates and products at the surface like formaldehyde, which is assumed to protect the Pt electrode, while the presence of CO at the Pt surface enhances dissolution.[37, 50] The formation of other products proposed for MOR in aqueous media, like formic acid and CO_2 are not considered here due to the absence of OH_{ad} species at the electrode in anhydrous methanol. Upon applying 0.9 V, formaldehyde and CO might be formed consecutively, meaning, that protective formaldehyde is formed first, but with time, more CO is produced, inducing Pt dissolution (see Eq. (1) and (2)). However, the increase of current density with time (Fig. 4b) seems to contradict the theory that formaldehyde is formed first, followed by the formation of CO, because CO would hinder methanol oxidation, leading to a decrease in current. It also seems possible that the increasing current and Pt dissolution stem from the increasing MOR rate due to accumulating oxygenated species at the surface and the removal of protective formaldehyde from the surface. The effect of the reaction products and intermediates on the stability of Pt electrodes is beyond the scope of this paper and is the subject of further investigations.

In the anhydrous acetonitrile electrolyte, Pt dissolution occurs at a constant rate at 0.9 V and the current density is very low (see Fig. 4d), indicating mainly non-faradaic processes. Direct dissolution seems to be the most obvious, i.e., Pt dissolves in the form of Pt ions, but also complex formation with MeCN might contribute to the constant dissolution rate. Harlow et al.[20] explained the displacement of water by complex formation of Pt with MeCN through the overlapping of MeCN π-orbitals with Pt d-orbitals. They found that in anhydrous MeCN, the surface expansion of Pt is around 3.4 % to 4.1 %, which could be weakening the Pt—Pt bonds and also have a promoting effect on Pt dissolution. A similar phenomenon was described earlier in metal carbonyl complexes, where a σ-bond is formed between a C-atom and a metal center. This bond is strengthened by the back donation of electrons in d-orbitals to antibonding π-orbitals.[51] It is worth noting that Marković et al.[52] described a surface lattice expansion of Pt of about 4 % in the presence of CO, which is similar to MeCN. The somewhat related Pt—CO and Pt—MeCN adsorption behavior, could also reflect in a similar Pt dissolution behavior, which would also help to elucidate Pt dissolution pathways during MOR and will be the subject of future investigations.

$$CH_3OH \rightarrow CH_2O + 2H^+ + 2e^- \quad (1)$$

$$CH_2O \rightarrow CO + 2H^+ + 2e^- \quad (2)$$

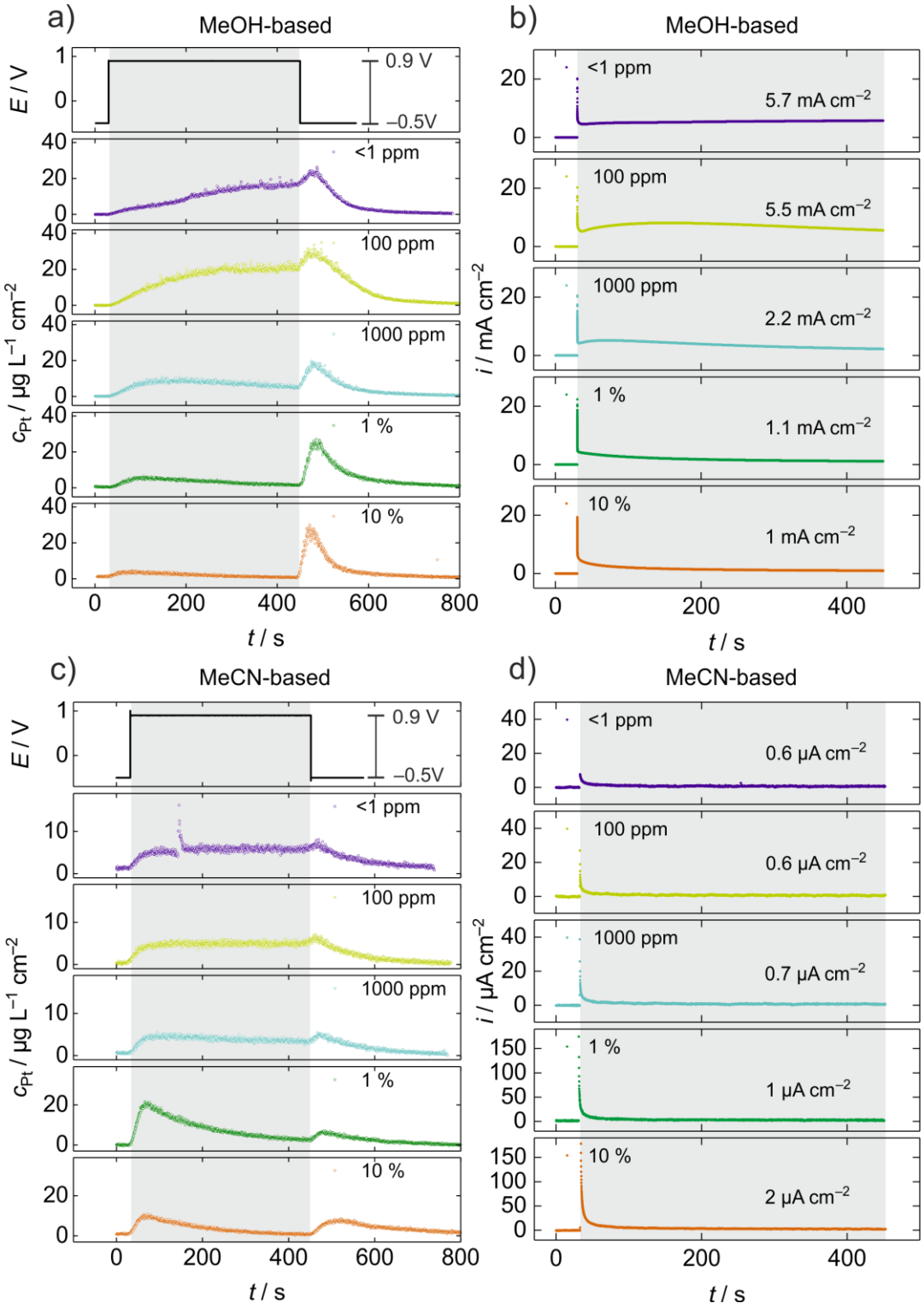

Fig. 4: Pt dissolution vs. time with different water contents (<1 ppm, 100 ppm, 1000 ppm, 1 %, 10 %) in a) 0.05 mol L^{-1} $LiClO_4$ containing MeOH and c) 0.05 mol L^{-1} $LiClO_4$ containing MeCN electrolytes and current density vs. time in b) 0.05 mol L^{-1} $LiClO_4$ containing MeOH and d) 0.05 mol L^{-1} $LiClO_4$ containing MeCN obtained during chronoamperometry at 0.9 V vs. Fc/Fc^+ for 7 min.

4. CONCLUSIONS

Using an electroanalytical flow cell coupled to an ICP-MS, we showed that controlled addition of water to two different nonaqueous electrolytes significantly influences the stability and electrochemical response of Pt electrodes. We analyzed MeOH-based and MeCN-based electrolytes and our experiments demonstrate that the presence of water in different concentrations (< 1 ppm, 100 ppm, 1000 ppm, 1 %, 10 %) results in different Pt dissolution profiles and mechanisms. In MeOH-based electrolytes, cathodic dissolution gradually develops, starting from a water content of 100 ppm, indicating that oxide species are formed at the Pt electrode surface. Additionally, it was found that the presence of 100 ppm water gave the highest current densities for methanol oxidation and further increases in water content shifted the onset potential of MOR to more negative values, further demonstrating the critical role of adsorbed oxide species for MOR. By contrast, in MeCN-based electrolytes, cathodic dissolution only appears at water concentrations of 1 % or higher during CVs. At the same time, it is much less pronounced, meaning that Pt oxide formation is largely hindered in MeCN due to strong solvent—metal interactions formed by solvent π-orbital complexation with metal d-orbitals. Major differences in Pt dissolution were also found during chronoamperometry in the anhydrous forms of electrolytes. Pt dissolution increases with electrolysis time in methanol, which indicates consecutive steps in the methanol oxidation mechanism involving formaldehyde and CO, the accumulation of oxygenated species at the surface or the removal of protective species from the surface. On the other hand, Pt dissolution stays constant in acetonitrile, which is explained by the oxidation of Pt to form Pt^{2+}, and possibly supported by Pt crystal lattice expansion upon adsorption of MeCN. Similarly to MeCN, CO can adsorb to the Pt surface in the case of methanol, leading to a comparable crystal lattice expansion and impairing the stability of Pt.

AUTHOR INFORMATION

Corresponding Authors

* E-mail: j.ranninger@fz-juelich.de
* E-mail: b.berkes@fz-juelich.de

Author Contributions

J.R. and B.B.B. planned, analyzed and discussed the experiments J.R. carried out the measurements and wrote the original draft. B.B.B. and K.J.J.M. reviewed and edited the manuscript.

Notes

The authors declare no competing financial interest.

ACKNOWLEDGMENTS

This work was supported by the German Research Foundation (DFG) under Germany's Excellence Strategy—Exzellenzcluster 2186 "The Fuel Science Center." The authors thank Jonas Möller for developing a LabVIEW software for EFC control and data evaluation and Pavlo Nikolaienko for valuable scientific discussions.

REFERENCES

1. Kwak, W. J.; Rosy; Sharon, D.; Xia, C.; Kim, H.; Johnson, L. R.; Bruce, P. G.; Nazar, L. F.; Sun, Y. K.; Frimer, A. A., et al. Lithium-Oxygen Batteries and Related Systems: Potential, Status, and Future. *Chem. Rev.* **2020,** *120,* 6626-6683.
2. Yoshida, J.-i.; Kataoka, K.; Horcajada, R.; Nagaki, A. Modern Strategies in Electroorganic Synthesis. *Chem. Rev.* **2008,** *108,* 2265–2299.
3. Yan, M.; Kawamata, Y.; Baran, P. S. Synthetic Organic Electrochemical Methods Since 2000: On the Verge of a Renaissance. *Chem. Rev.* **2017,** *117,* 13230-13319.
4. Staszak-Jirkovský, J.; Subbaraman, R.; Strmcnik, D.; Harrison, K. L.; Diesendruck, C. E.; Assary, R.; Frank, O.; Kobr, L.; Wiberg, G. K. H.; Genorio, B., et al. Water as a Promoter and Catalyst for Dioxygen Electrochemistry in Aqueous and Organic Media. *ACS Catal.* **2015,** *5,* 6600-6607.
5. Lu, Y. C.; Gasteiger, H. A.; Shao-Horn, Y. Catalytic Activity Trends of Oxygen Reduction Reaction for Nonaqueous Li-Air Batteries. *J. Am. Chem. Soc.* **2011,** *133,* 19048-19051.
6. Laoire, C. O.; Mukerjee, S.; Abraham, K. M. Influence of Nonaqueous Solvents on the Electrochemistry of Oxygen in the Rechargeable Lithium-Air Battery. *J. Phys. Chem. C* **2010,** *114,* 9178–9186.
7. Aldous, I. M.; Hardwick, L. J. Solvent-Mediated Control of the Electrochemical Discharge Products of Non-Aqueous Sodium-Oxygen Electrochemistry. *Angew. Chem. Int. Ed.* **2016,** *55,* 8254-8257.
8. Agyeman, D. A.; Zheng, Y.; Lee, T.-H.; Park, M.; Tamakloe, W.; Lee, G.-H.; Jang, H. W.; Cho, K.; Kang, Y.-M. Synergistic Catalysis of the Lattice Oxygen and Transition Metal Facilitating ORR and OER in Perovskite Catalysts for Li–O_2 Batteries. *ACS Catal.* **2021,** *11,* 424-434.
9. Suarez-Herrera, M. F.; Costa-Figueiredo, M.; Feliu, J. M. Voltammetry of Basal Plane Platinum Electrodes in Acetonitrile Electrolytes: Effect of the Presence of Water. *Langmuir* **2012,** *28,* 5286-5294.
10. Ledezma-Yanez, I.; Díaz-Morales, O.; Figueiredo, M. C.; Koper, M. T. M. Hydrogen Oxidation and Hydrogen Evolution on a Platinum Electrode in Acetonitrile. *ChemElectroChem* **2015,** *2,* 1612-1622.
11. Dubouis, N.; Serva, A.; Salager, E.; Deschamps, M.; Salanne, M.; Grimaud, A. The Fate of Water at the Electrochemical Interfaces: Electrochemical Behavior of Free Water Versus Coordinating Water. *J. Phys. Chem. Lett.* **2018,** *9,* 6683-6688.
12. Dubouis, N.; Serva, A.; Berthin, R.; Jeanmairet, G.; Porcheron, B.; Salager, E.; Salanne, M.; Grimaud, A. Tuning Water Reduction Through Controlled Nanoconfinement Within an Organic Liquid Matrix. *Nat. Catal.* **2020,** *3,* 656-663.
13. Rudnev, A. V.; Molodkina, E. B.; Danilov, A. I.; Polukarov, Y. M.; Berna, A.; Feliu, J. M. Adsorption Behavior of Acetonitrile on Platinum and Gold Electrodes of Various Structures in Solution of 0.5 M H_2SO_4. *Electrochim. Acta* **2009,** *54,* 3692-3699.
14. Pemberton, J. E.; Joa, S. L. Water and Electrolyte Structure at Ag Electrodes in Nonaqueous Butanol Solutions Using Surface-Enhanced Raman Scattering *J. Electroanal. Chem.* **1994,** *378,* 149-158.
15. Feng, G.; Qiao, X. J. R.; Kornyshev, A. A. Water in Ionic Liquids at Electrified Interfaces: The Anatomy of Electrosorption. *ACS Nano* **2014,** *8,* 11685–11694.
16. Więckowski, A. The Classification of Adsorption Processes of Organic Compounds on Platinum Electrode. The Role of Water Molecules Chemisorbed on Platinum. *Electrochim. Acta* **1981,** *26,* 1121-1124.
17. Angerstein-Kozlowska, H.; MacDougall, B.; Conway, B. E. Electochemisorption and Reactivity of Nitriles at a Platinum Electrodes and the Anodic H Desorption Effect. *J. Electroanal. Chem.* **1972,** *39,* 287-313.
18. Barrett, P.; Pruszkowska, E. Use of Organic Solvents for Inductively Coupled Plasma Analyses. *Anal. Chem.* **1984,** *56,* 1927-1930.
19. Morin, S.; Conway, B. E.; Edens, G. J.; Weaver, M. J. The Reactive Chemisorption of Acetonitrile on Pt(111) and Pt(100) Electrodes as Examined by *in situ* Infrared Spectroscopy. *J. Electroanal. Chem.* **1997,** *421,* 213-220.
20. Harlow, G. S.; Aldous, I. M.; Thompson, P.; Grunder, Y.; Hardwick, L. J.; Lucas, C. A. Adsorption, Surface Relaxation and Electrolyte Structure at Pt(111) Electrodes in Non-Aqueous and Aqueous Acetonitrile Electrolytes. *Phys. Chem. Chem. Phys.* **2019,** *21,* 8654-8662.
21. Morin, S.; Conway, B. E. Surface Structure Dependence on Single-Crystal Pt Surfaces. *J. Electroanal. Chem.* **1994,** *376,* 135-150.

22. Krtil, P.; Kavan, L.; Novák, P. Oxidation of Acetonitrile-Based Electrolyte Solutions at High Potentials: An *In Situ* Fourier Transform Infrared Spectroscopy Study. *J. Electrochem. Soc.* **1993,** *140,* 3390.
23. Cao, P.; Sun, Y.; Gu, R. On the Occurrence of Competitive Adsorption at the Platinum-Acetonitrile Interface by Using Surface-Enhanced Raman Spectroscopy. *J. Phys. Chem. B* **2003,** *107,* 5818-5824.
24. Cao, P.; Sun, Y.; Gu, R. Investigations of Chemisorption and Reaction at Non-Aqueous Electrochemical Interfaces by *in situ* Surface-Enhanced Raman Spectroscopy. *J. Raman Spectrosc.* **2005,** *36,* 725-735.
25. Baldelli, S.; Mailhot, G.; Ross, P.; Shen, Y.-R.; Somorjai, G. A. Potential Dependent Orientation of Acetonitrile on Platinum (111) Electrode Surface Studied by Sum Frequency Generation. *J. Phys. Chem. B* **2001,** *105,* 654-662.
26. Pons, S.; Khoo, S. B. Reductions in Aprotic Media-I. Cathodic Reduction Limits at a Platinum Electrode in Acetonitrile. *Electrochim. Acta* **1982,** *27,* 1161-1169.
27. Foley, J. K.; Korzeniewski, C.; Pons, S. Anodic and Cathodic Reactions in Acetonitrile/Tetra-*n*-butylammonium tetrafluoroborate: an Electrochemical and Infrared Spectroelectrochemical Study. *Can. J. Chem.* **1988,** *66,* 201-206.
28. Portis, L. C.; Roberson, J. C.; Mann, C. K. Anodic Background Reaction in Moist Acetonitrile. *Anal. Chem.* **1972,** *44,* 294-297.
29. Gilman, S.; Breiter, M. W. Anodic Oxidation of Methanol on Platinum: II . Interpretation of Potentiostatic Current-Potential Curves in Acidic Solution. *J. Electrochem. Soc.* **1962,** *109,* 1099.
30. Bagotzky, V. S.; Vassiliev, Y. B.; Khazova, O. A. Generalized Scheme of Chemisorption, Electrooxidation and Electroreduction of Simple Organic Compounds on Platinum Group Metals. *J. Electroanal. Chem.* **1977,** *81,* 229-238.
31. Batista, E. A.; Malpass, G. R. P.; Motheo, A. J.; Iwasita, T. New Mechanistic Aspects of Methanol Oxidation. *J. Electroanal. Chem.* **2004,** *571,* 273-282.
32. Romano, R. L.; Oliveira, M. G.; Varela, H. The Impact of Water Concentration on the Electro-Oxidation of Methanol on Platinum. *J. Electrochem. Soc.* **2020,** *167,* 046506.
33. Ranninger, J.; Wachs, S. J.; Möller, J.; Mayrhofer, K. J. J.; Berkes, B. B. On-line Monitoring of Dissolution Processes in Nonaqueous Electrolytes – A Case Study with Platinum. *Electrochem. Commun.* **2020,** *114,* 106702.
34. Jerkiewicz, G.; Vatankhah, G.; Lessard, J.; Soriaga, M. P.; Park, Y.-S. Surface-Oxide Growth at Platinum Electrodes in Aqueous H_2SO_4. *Electrochim. Acta* **2004,** *49,* 1451-1459.
35. Sugawara, Y.; Okayasu, T.; Yadav, A. P.; Nishikata, A.; Tsuru, T. Dissolution Mechanism of Platinum in Sulfuric Acid Solution. *J. Electrochem. Soc.* **2012,** *159,* F779-F786.
36. Topalov, A. A.; Katsounaros, I.; Auinger, M.; Cherevko, S.; Meier, J. C.; Klemm, S. O.; Mayrhofer, K. J. Dissolution of Platinum: Limits for the Deployment of Electrochemical Energy Conversion? *Angew. Chem. Int. Ed.* **2012,** *51,* 12613-12615.
37. Ranninger, J.; Nikolaienko, P.; Wachs, S. J.; Möller, J.; Mayrhofer, K. J. J.; Berkes, B. B. Dissolution of Pt and Its Temperature Dependence in Anhydrous Acetonitrile- and Methanol-Based Electrolytes. *J. Electrochem. Soc.* **2020,** *167,* 121507.
38. Pavlishchuk, V. V.; Addison, A. W. Conversion Constants for Redox Potentials Measured Versus Different Reference Electrodes in Acetonitrile Solutions at 25°C. *Inorg. Chim. Acta* **2000,** *298,* 97-102.
39. Boorn, A. W.; Browner, R. F. Effects of Organic Solvents in Inductively Coupled Plasma Atomic Emission Spectrometry. *Anal. Chem.* **1982,** *54,* 1402-1414.
40. Hutton, R. C. Application of Inductively Coupled Plasma Source Mass Spectrometry (ICP-MS) to the Determination of Trace Metals in Organics. *J. Anal. At. Spectrom.* **1986,** *1,* 259-263.
41. Jovanovič, P.; Šelih, V. S.; Šala, M.; Hočevar, S.; Ruiz-Zepeda, F.; Hodnik, N.; Bele, M.; Gaberšček, M. Potentiodynamic Dissolution Study of PtRu/C Electrocatalyst in the Presence of Methanol. *Electrochim. Acta* **2016,** *211,* 851-859.
42. Kormányos, A.; Speck, F. D.; Mayrhofer, K. J. J.; Cherevko, S. Influence of Fuels and pH on the Dissolution Stability of Bifunctional PtRu/C Alloy Electrocatalysts. *ACS Catal.* **2020,** *10,* 10858-10870.
43. Iwasita, T. Electrocatalysis of Methanol Oxidation. *Electrochim. Acta* **2002,** *47,* 3663-3674.
44. Gasteiger, H. A.; Markovic , N. M.; Ross, P. N. Methanol Electrooxidation on Well-Characterized Pt-Ru Alloys. *J. Phys. Chem.* **1993,** *97,* 12020-12029.
45. Christensen, P. A.; Hamnett, A.; L., T. G. The Role of Morphology in the Methanol Electro-Oxidation Reaction. *J. Electroanal. Chem.* **1993,** *362,* 207-218.
46. Iwasita, T.; Xia, X. H.; Liess, H.-D.; Vielstich, W. Electrocatalysis of Organic Oxidations: Influence of Water Adsorption on the Rate of Reaction. *J. Phys. Chem. B* **1997,** *101,* 7542-7547.
47. Zhao, Y.; Li, X.; Schechter, J. M.; Yang, Y. Revisiting the Oxidation Peak in the Cathodic Scan of the Cyclic Voltammogram of Alcohol Oxidation on Noble Metal Electrodes. *RSC Adv.* **2016,** *6,* 5384-5390.
48. Shayeghi, A.; Krähling, S.; Hörtz, P.; Johnston, R. L.; Heard, C. J.; Schäfer, R. Adsorption of Acetonitrile, Benzene, and Benzonitrile on Pt(111): Single Crystal Adsorption Calorimetry and Density Functional Theory. *J. Phys. Chem. C* **2017,** *121,* 21354-21363.
49. Karp, E. M.; Silbaugh, T. L.; Crowe, M. C.; Campbell, C. T. Energetics of Adsorbed Methanol and Methoxy on Pt(111) by Microcalorimetry. *J. Am. Chem. Soc.* **2012,** *134,* 20388-20395.
50. Topalov, A. A.; Zeradjanin, A. R.; Cherevko, S.; Mayrhofer, K. J. J. The Impact of Dissolved Reactive Gases on Platinum Dissolution in Acidic Media. *Electrochem. Commun.* **2014,** *40,* 49-53.
51. Blyholder, G. Molecular Orbital View of Chemisorbed Carbon Monoxide. *J. Phys. Chem.* **1964,** *68,* 2772-2777.
52. Marković, N. M.; Jr., P. N. R. Surface Science Studies of Model Fuel Cell Electrocatalysts. *Surf. Sci. Rep.* **2002,** *45,* 117-229.

TOC Graphic

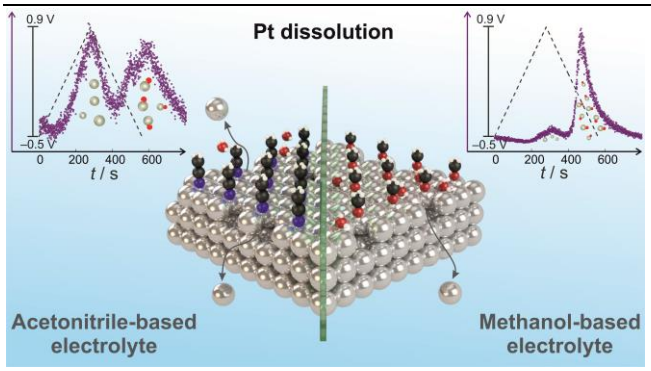
Pt dissolution
0.9 V
−0.5 V
0
200
400
600
t / s
0.9 V
−0.5 V
0
200
400
600
t / s
Acetonitrile-based electrolyte
Methanol-based electrolyte